

Interactions between aerosol organic components and liquid water content during haze episodes in Beijing

Xiaoxiao Li¹, Shaojie Song², Wei Zhou¹, Jiming Hao¹, Douglas R. Worsnop^{3,4}, and Jingkun Jiang^{1*}

¹State Key Joint Laboratory of Environment Simulation and Pollution Control, School of Environment, Tsinghua University, Beijing, 100084, China

²School of Engineering and Applied Sciences, Harvard University, Cambridge, Massachusetts 02138, USA

³Institute for Atmospheric and Earth System Research / Physics, Faculty of Science, University of Helsinki, Finland

⁴Aerodyne Research Inc., Billerica, Massachusetts 01821, USA

*: Correspondence to: J. Jiang (jiangjk@tsinghua.edu.cn)

Abstract: Aerosol liquid water (ALW) is ubiquitous in ambient aerosol and plays an important role in the formation of both aerosol organics and inorganics. To investigate the interactions between ALW and aerosol organics during haze formation and evolution, ALW was modelled based on long-term measurement of submicron aerosol composition in different seasons in Beijing. ALW contributed by aerosol inorganics (ALW_{inorg}) was modelled by ISORROPIA-II, and ALW contributed by organics (ALW_{org}) was estimated with κ -Köhler theory, where real-time hygroscopicity parameter of the organics (κ_{org}) was calculated from the real-time organic oxygen-to-carbon ratio (O/C). Overall particle hygroscopicity (κ_{total}) was computed by weighting component hygroscopicity parameters based on their volume fractions in the mixture. We found that ALW_{org} , which is often neglected in traditional ALW modelling, contributes a significant fraction (18-32%) to the total ALW in Beijing. The ALW_{org} fraction is largest in the cleanest days when both the organic fraction and κ_{org} are relatively high. The large variation of O/C, from 0.2 to 1.3, indicates the wide variety of organic components. This emphasizes the necessity of using real-time κ_{org} , instead fixed κ_{org} , to calculate ALW_{org} in Beijing. The significant variation of κ_{org} (calculated from O/C), together with highly variable organic or inorganic volume fractions, leads to a wide range of κ_{total} (between 0.20 and 0.45), which has great impact on water uptake. The variation of organic O/C, or derived κ_{org} , was found to be influenced by temperature (T), ALW, and aerosol mass concentrations, among which, T and ALW both have promoting effects on O/C. During high-ALW haze episodes, although the organic fraction decreases rapidly, O/C, and derived κ_{org} , increase with the increase in ALW, suggesting the formation of more soluble organics via heterogeneous uptake or aqueous processes. A positive feedback loop is thus formed: during high-ALW episodes, increasing κ_{org} , together with decreasing particle organic fraction (or increasing particle inorganic fraction), increases κ_{total} , thus further promotes the ability of particles to uptake water.

1 INTRODUCTION

Aerosol liquid water (ALW) is a ubiquitous component of ambient aerosol and exerts great influences on aerosol physical and chemical properties, especially in regions with high relative humidity (RH) (Cheng et al., 2016; Cheng et al., 2008; Covert et

33 al., 1972; Ervens et al., 2014; Nguyen et al., 2016; Pilinis et al., 1989; Wu et al., 2018; Zheng et al., 2015). From the perspective
34 of aerosol physical processes, ALW influences particle lifetime, optical properties, radiative forcing, and the ability of particles
35 to deposit in the humid human respiratory tract (Andreae and Rosenfeld, 2008; Cheng et al., 2008; Covert et al., 1972; Löndahl
36 et al., 2008). ALW also promotes partitioning of some of the inorganic gases and water-soluble organic gases to the condensed
37 phase, thus directly increasing aerosol mass loadings (Asa-Awuku et al., 2010; Parikh et al., 2011). From the perspective of
38 aerosol chemical processes, ALW can serve as a reactor for heterogeneous/aqueous reactions, facilitating the formation of both
39 secondary inorganics (Cheng et al., 2016; Sievering et al., 1991; Wang et al., 2016) and organics (Carlton et al., 2009; Ervens
40 et al., 2014; Song et al., 2019). As a result, understanding ALW content is critical in clarifying the formation and evolution of
41 ambient aerosols as well as their impacts on air quality and climate, especially in urban cities like Beijing where severe haze
42 events take place frequently with elevated RH (Sun et al., 2013; Zheng et al., 2015).

43
44 The interaction between ALW and aerosol chemical composition is a key issue for haze formation but remains uncertain,
45 especially regarding the interaction between ALW and aerosol organics. Studies have demonstrated that secondary inorganic
46 aerosol (SIA) and secondary organic aerosol (SOA) surpass primary species during haze formation in China (Huang et al.,
47 2014; Sun et al., 2016; Zheng et al., 2016). SOA or SIA-driven haze formation is widely observed to be associated with elevated
48 relative humidity (RH), especially in winter. In Beijing, as RH rises from below 40% to above 60%, the following has been
49 reported: (1) aerosol mass loadings increase significantly; (2) particle phase changes from solid/semisolid to liquid phase (Liu
50 et al., 2017); (3) both sulfur and nitrogen oxidation ratios increase (Cheng et al., 2016; Sun et al., 2013; Zheng et al., 2015);
51 (4) water-soluble inorganics increase faster than organics (Liu et al., 2015; Quan et al., 2015; Sun et al., 2013; Zheng et al.,
52 2015). RH affects secondary species via heterogeneous uptake or aqueous processes. During haze episodes, gas phase
53 photochemical formation of SIA and SOA is largely suppressed by the weakened solar radiation (Zheng et al., 2015). Formation
54 of SIA and SOA is thus suggested to be dominated by heterogeneous uptake or aqueous processes (Xu et al., 2017), which are
55 largely dependent on ALW. Based on ALW measurements, previous studies have proposed positive feedback loops in which
56 elevated RH increases particle concentration and particle inorganic fraction; increased particle concentration and inorganic
57 fraction in turn increase the water uptake (Cheng et al., 2016; Liu et al., 2017; Wu et al., 2018). However, whether or how
58 elevated ALW affects the evolution of SOA during haze episodes remains less understood than that of SIA because of the
59 complexity of SOA species.

60
61 Long-term data are needed to evaluate the amount of ALW and its interactions with aerosol organic compositions. So far, short-
62 term ALW data in Beijing (Bian et al., 2014; Fajardo et al., 2016) have been collected by directly measuring size-resolved
63 aerosol hygroscopic volume growth factors (VGF) and particle size distributions using hygroscopicity-tandem differential
64 mobility analyzer (H-TDMA) (Rader and McMurry, 1986) or dry-ambient aerosol size spectrometer (DAASS) (Engelhart et

65 al., 2011; Stanier et al., 2004). However, long-term measurements of ALW are rare because of the challenge in maintaining
66 these instruments. Another approach to obtain ALW is to combine aerosol chemical composition measurements and model
67 predictions. ALW contributed by inorganics can be modelled by inorganic thermodynamic equilibrium models, such as
68 ISORROPIA-II (Fountoukis and Nenes, 2007; Nenes et al., 1998, 1999), E-AIM (Clegg and Pitzer, 1992; Clegg et al., 1992),
69 and SCAPE II (Kim et al., 1993a, b). Modelled inorganic water content is usually regarded as the total ALW because inorganic
70 salts contribute to a large fraction of the total particle loading and the hygroscopicity of inorganic salts is much larger (~6
71 times) than those of organic species (Bian et al., 2014; Hennigan et al., 2008). Although this approximation provides reasonable
72 ALW in many ambient conditions, it fails in some cases. Especially when organics contribute a dominant fraction to particle
73 loading, large discrepancies arise between the modelled inorganic water and the actual ALW content (Fajardo et al., 2016).
74 Therefore, it is important to take the organic contribution to ALW into consideration. Some specific models include the
75 calculation of organic ALW; e.g., aerosol diameter dependent equilibrium model (ADDEM)(Topping et al., 2005b, a). However,
76 application of such models is hindered by lack of long-term measurements of specific OA species.

77
78 Recent studies have proposed a method to predict total ALW using the non-refractory submicron particulate matter (NR-PM₁,
79 particle diameter between 40 nm and 1 μm) composition measured with the widely used Aerosol Mass Spectrometer (AMS).
80 The inorganic contribution to ALW (ALW_{inorg}) was modelled by ISORROPIA-II; organic contribution to ALW (ALW_{org}) was
81 estimated with κ-Köhler theory (Petters and Kreidenweis, 2007; Su et al., 2010). The total aerosol liquid water (ALW) is then
82 the sum of ALW_{inorg} and ALW_{org}. ALW estimated by this method, which only requires aerosol chemical composition obtained
83 from AMS measurements (Zhang et al., 2007), corresponds reasonably with measured ALW (The ratio of predicted ALW to
84 measured ALW is 0.91, with R² = 0.75) (Guo et al., 2015). Thus, this method can be used to predict long-term ALW from
85 aerosol chemical composition and to explore interactions between ALW and organic evolution during haze events.

86
87 In this study, long-term NR-PM₁ chemical composition measurement was used to predict ALW in Beijing during various
88 seasons (292 days in 5 years). ALW_{org} and ALW_{inorg} were estimated using κ-Köhler theory and ISORROPIA-II, respectively. A
89 real-time organic hygroscopic parameter (κ_{org}, calculated from organic O/C ratio) was used to estimate ALW_{org}. The
90 relationship between the total ALW and κ_{org} was explored. Within this long-term dataset, 12 high-ALW haze episodes and 8
91 low-ALW haze episodes were identified. Chemical evolution during high-ALW and low-ALW haze episodes was found to
92 differ significantly. Positive feedback among organic hygroscopicity, organic volume fraction, overall particle hygroscopicity,
93 and ALW is proposed to be a driving factor for severe haze formation in Beijing during high-ALW episodes.

95 **2.1 Long-term measurements of particle chemical composition**

96 Long-term measurements were carried out between December 2013 and August 2017 at an urban site located on the campus
97 of Tsinghua University in Beijing. The monitoring site is located on the top floor of a four-storey building without other tall
98 buildings nearby with detailed information provided elsewhere (Cai and Jiang, 2017; Cao et al., 2014; He et al., 2001). Data
99 from 292 days were used, including 2-3 months' data from each of the four seasons (Table S1). The average NR-PM₁ mass
100 concentrations from spring to winter were 81.1, 54.2, 63.9, and 63.2 μg m⁻³, respectively. Note that PM_{2.5} concentrations in
101 Beijing were decreasing during this period (<http://www.bjepb.gov.cn/>).

102

103 Chemical composition of NR-PM₁, including sulfate (SO₄²⁻), nitrate (NO₃⁻), ammonium (NH₄⁺), chloride (Cl⁻), and total
104 organics (Org), was measured using a quadrupole aerosol chemical speciation monitor (Q-ACSM)(Ng et al., 2011). The Q-
105 ACSM was calibrated before each measurement following the procedure described by Ng et al., (2011). The meteorological
106 conditions, including temperature (*T*), relative humidity (RH), and other routine meteorological parameters, were recorded by
107 a meteorological station.

108 **2.2 Aerosol liquid water modelling**

109 ALW_{inorg} was modelled by ISORROPIA-II using meteorological conditions and the Q-ACSM measured inorganic
110 compositions. The model was carried out with “reverse” and “metastable” mode. Compared to the “stable” mode, “metastable”
111 mode assumes that particles are always aqueous droplets, even at low RH. Although some earlier studies observed phase
112 transitions of ambient particles, recent studies suggest that ambient aerosols tend to be in “metastable” states due to the
113 coexistence of organic compounds that inhibit or cover up the deliquescence and efflorescence behavior of inorganic
114 compounds (Martin et al., 2008; Rood et al., 1989). The “metastable” mode predicts more water than predicted from “stable”
115 mode when RH is between 40% and 70%, while similar with the latter when RH is above 70% or below 40% (Fig. S1),
116 consistent with previous work (Song et al., 2018). In a few of the modelling results in summer and autumn, high acid/base
117 ratio caused some of the NO₃⁻ and Cl⁻ to enter the gas phase in the form of HNO₃ and HCl, resulting in disagreement between
118 the output liquid phase NO₃⁻ and Cl⁻ and the input aerosol phase NO₃⁻ and Cl⁻. These points were removed.

119

120 ALW_{org} was estimated using a simplified equation of κ-Köhler theory where Kelvin effect was neglected (Petters and
121 Kreidenweis, 2007) (Eq. 1),

122
$$ALW_{org} = V_{org} \kappa_{org} \frac{a_w}{1-a_w} \quad (1)$$

123 where a_w is the water activity and was assumed to be the same as RH (Bassett and Seinfeld, 1983) and V_{org} is the volume
 124 concentration of organics measured by Q-ACSM (the density of organics was assumed to be 1.2 g cm^{-3}). In previous studies,
 125 a fixed κ_{org} in the range of 0.06-0.13 was used for urban, urban downwind, and rural sites (Gunthe et al., 2011; Nguyen et al.,
 126 2016; Rose et al., 2011). However, the hygroscopicity of organics is highly variable and κ_{org} can vary between 0 and 0.3 for
 127 different species (Lambe et al., 2011; Massoli et al., 2010). κ_{org} was found to have a positive linear relationship with organic
 128 O/C ratio (Chang et al., 2010; Dick et al., 2000; Duplissy et al., 2011; Gunthe et al., 2011; Petters et al., 2009), which likely
 129 reflects combined effects of molecular weight, volatility, and surface activity (Nakao, 2017; Wang et al., 2019). Previous
 130 studies proposed several empirical methods to calculate κ_{org} from O/C derived from a series of chamber and field experiments
 131 (Chang et al., 2010; Duplissy et al., 2011; Jimenez et al., 2009; Lambe et al., 2011; Massoli et al., 2010). Comparing these
 132 methods (Table S2), Eq. 2 was used to calculate real-time κ_{org} over a broad O/C range (0.05-1.42) (Lambe et al., 2011),

$$133 \quad \kappa_{org} = (0.18 \pm 0.04) \times O/C + 0.03 \quad (2)$$

134 where real-time O/C was calculated from Q-ACSM measured f_{44} (the fraction of m/z 44 fragments signal to total organic signal,
 135 $O/C = 0.079 + 4.31 \times f_{44}$) which has been widely used to study the aging process of OA species (Canagaratna et al., 2015; Ng
 136 et al., 2010).

137
 138 The Zdanovskii-Stokes-Robinson (ZSR) mixing rule was used to calculate the total ALW. According to ZSR, the total water
 139 uptake into internally mixed particles is the sum of water content uptake by each pure component (Jing et al., 2018).

140
 141 Particle hygroscopic volume growth factor (VGF) is the ratio of the volume of the wet particle to the corresponding particle
 142 volume at dry conditions. The size-independent VGF was calculated using Eq. 3,

$$143 \quad \text{VGF} = \frac{\sum \frac{m_{i,ACSM}}{\rho_i} + (ALW_{inorg} + ALW_{org})/\rho_{water}}{\sum \frac{m_{i,ACSM}}{\rho_i}} \quad (3)$$

144 where $m_{i,ACSM}$ is the mass concentration of species “i” measured by Q-ACSM. The densities were assumed to be 1.75, 1.75,
 145 1.75, 1.52, 1.2, and 1.0 g cm^{-3} for sulfate, nitrate, ammonium, chloride, organics, and water, respectively (Salcedo et al., 2006).

146
 147 Overall particle hygroscopicity (κ_{total}) was calculated by weighting component hygroscopicity parameters by their volume
 148 fractions in the mixture (Dusek et al., 2010; Gunthe et al., 2009; Petters and Kreidenweis, 2007) (Eq. 4),

$$149 \quad \kappa_{total} = \kappa_{inorg} \cdot \text{frac}_{inorg} + \kappa_{org} \cdot \text{frac}_{org} \quad (4)$$

150 where frac_{inorg} and frac_{org} are the inorganic and organic volume fractions in NR-PM₁, respectively. Inorganic species are mainly
 151 in the form of NH_4NO_3 , H_2SO_4 , NH_4HSO_4 , and $(\text{NH}_4)_2\text{SO}_4$ (Liu et al., 2014); corresponding hygroscopic parameters were
 152 0.68, 0.68, 0.56, and 0.52, respectively. As a result, an average value of 0.6 was used as the hygroscopicity parameter of the
 153 inorganic components (κ_{inorg}), with the assumption that the relative abundance of NH_4NO_3 , H_2SO_4 , NH_4HSO_4 , and $(\text{NH}_4)_2\text{SO}_4$

154 does not change significantly. Thus in our study, variation of κ_{total} with RH only reflects changes in $frac_{org}$ and κ_{org} .

155 **2.3 Haze episode identification**

156 The haze pollution in Beijing have shown typical evolution pattern where a pollution episode usually starts with a clean day,
157 then accumulates for 2-7 days, and eventually disappears within 1-2 days (Guo et al., 2014; Jia et al., 2008; Zheng et al., 2016).
158 In this study, 22 haze episodes were identified (Table S3). Only episodes containing 4 or more than 4 calendar days were taken
159 into consideration. The haze episodes were further classified according to ALW volume fraction; that is, the ratio of ALW
160 volume to the wet particle total volume (ALW volume fraction = $V_{ALW} / (V_{ALW} + V_{NR-PM1})$). 12 were distinguished as high-
161 ALW haze episodes (ALW volume fraction > 0.3 for at least 50% of the haze period), while 8 were distinguished as low-ALW
162 haze episodes. All 20 distinguished episodes were associated with growing RH, the other 2 with irregular RH variations were
163 classified as undefined. Average NR-PM₁ mass concentrations for the high-ALW and low-ALW episodes were 100.8 $\mu\text{g m}^{-3}$
164 and 76.2 $\mu\text{g m}^{-3}$, respectively.

165
166 The relative daily increments of $frac_{org}$, κ_{org} , $\kappa_{org} \cdot frac_{org}$ (indicates the contribution of organics to κ_{total}), and κ_{total} during the
167 classified 12 high-ALW haze episodes and 8 low-ALW haze episodes were averaged separately. Daily increments were used,
168 rather than hourly increments, to avoid the impact of diurnal variability. The first and last day of the episodes were not included
169 in the analysis as they were usually clean days, so that the chemical evolution was different from the hazy days. To minimize
170 the influence of transport or large local primary emissions, the relative κ_{org} daily increments of more than 40% were not
171 included in further analysis.

172 **3. RESULTS AND DISCUSSION**

173 **3.1 Aerosol liquid water contributed by organics**

174 The contribution of ALW_{org} to ALW is the highest when NR-PM₁ mass concentrations are below 25 $\mu\text{g m}^{-3}$. In this low mass
175 loading, ALW_{org}/ALW varies widely between ~10% and ~80%, with an average of 32% (Fig. 1a). The high ALW_{org}/ALW in
176 low aerosol mass concentrations can be explained by high organics/NR-PM₁ mass fractions ($57 \pm 15\%$) (as shown in Fig. 1b)
177 and high κ_{org} (as shown in Fig. 2). The striking variability in ALW_{org}/ALW is the result of highly variable chemical
178 compositions during clean days. In addition, higher uncertainties in NR-PM₁ measurements of low NR-PM₁ loadings and in
179 ALW modelling at low RH may also contribute to the large variability. High ALW_{org}/ALW in low aerosol mass concentrations
180 is consistent with previous studies (Dick et al., 2000; Fajardo et al., 2016). Those studies showed that modelled ALW_{inorg} was
181 much lower than measured total ALW under low aerosol mass loadings in Beijing (Fajardo et al., 2016) and that ALW_{org} was

182 comparable to ALW_{inorg} in low RH (Dick et al., 2000).

183

184 As NR- PM_1 mass concentrations increase from below $25 \mu g m^{-3}$ to above $100 \mu g m^{-3}$, average ALW_{org}/ALW fraction decreases
185 from an average of 32% to 18% in Beijing (Fig. 1a). This decrease is mainly caused by the decrease of organics/NR- PM_1 mass
186 fractions from an average of 57% to 34% (Fig. 1b), and the decrease in organic/NR- PM_1 correlates with elevated RH, as
187 indicated by the color of the scattered points. Although organic concentration increases with rising RH and NR- PM_1 , the
188 concentration of inorganic water-soluble salts increases even more, leading to a decreased fraction of organics. Variation of
189 ALW_{org}/ALW narrows as NR- PM_1 mass concentration increase. During high aerosol concentration, the aerosols are aged and
190 dominated by secondary species (Huang et al., 2014); while during low concentration, the origins of aerosol are more complex
191 and variable. As a result, the chemical composition of NR- PM_1 become more homogeneous with the increase in NR- PM_1 .

192

193 ALW_{org} calculated using the real-time κ_{org} is much higher than that using a fixed κ_{org} (0.08), which has often been used to
194 represent the hygroscopicity of urban organic aerosols (Nguyen et al., 2016). However, κ_{org} in Beijing varies remarkably
195 between 0.06 and 0.26, with an average of 0.16 ± 0.04 , much higher than 0.08. This higher κ_{org} results in a higher ALW_{org}
196 fraction (18-32%) calculated in our study than predicted in previous ones (Nguyen et al., 2016; Wu et al., 2018). We note
197 higher κ_{org} could be introduced via the conversion from organic O/C (Eq. 2); though κ_{org} calculated from others
198 parameterizations (Chang et al., 2010; Duplissy et al., 2011; Massoli et al., 2010; Peter et al., 2006; Raatikainen et al., 2010)
199 are even higher than from the one used here (Fig. S2). As shown in Table. S2, the average κ_{org} calculated from other methods
200 are 0.22 ± 0.07 (Chang et al., 2010), 0.19 ± 0.06 (Massoli et al., 2010), and 0.21 ± 0.08 (Duplissy et al., 2011; Jimenez et al.,
201 2009). Also, based on previous reports that Q-ACSM can report higher f_{44} values than the HR-ToF-AMS (Fröhlich et al., 2015)
202 and that f_{44} reported by Q-ACSM may be highly variable among different instruments (Crenn et al., 2015), there is a possibility
203 that positive deviations and large uncertainties of f_{44} were introduced via the Q-ACSM measurements. Despite these
204 possibilities, the large variations in κ_{org} emphasize the need to use real-time κ_{org} instead of a fixed value. When real-time κ_{org} is
205 not available, at least a localized average κ_{org} for a given site should be considered.

206 3.2 Influence of temperature, ALW, and NR- PM_1 mass concentrations on organic hygroscopicity

207 Organic O/C ratio and the derived organic hygroscopicity increase with an increase in the ambient temperature for all the four
208 seasons (Fig. 2). This positive correlation is more significant when T is below $15 \text{ }^\circ\text{C}$. For the different seasons, average O/C
209 ratios for summer, spring, autumn, and winter are 0.96, 0.82, 0.70, and 0.55, with corresponding average T of 27.6, 14.6, 10.0,
210 and $2.3 \text{ }^\circ\text{C}$, respectively. Diurnally, organic O/C show clear peaks at 14:00-16:00 which matches the diurnal variation of T well
211 (Fig. S3). Similar diurnal changes of organic O/C have been previously observed (Hu et al., 2016; Sun et al., 2016). The
212 promoting effect of T on O/C can be attributed to multiple processes. On one hand, T often correlates with higher solar radiation

213 and higher atmospheric oxidative capacity. On the other hand, higher T accelerates gas phase and heterogeneous uptake or
214 aqueous processes and thus increases O/C. In addition, higher T promotes the partitioning of semi-volatile species (usually
215 less oxidized than low-volatile species) from particle phase to gas phase, also resulting in an increase in particle organic O/C.

216
217 Fig. 3 shows the influence of ALW and NR-PM₁ mass concentration on organic O/C, and organic hygroscopicity. The cross-
218 impact of T to O/C was separated by looking at the same color in Fig. 3. When ALW volume fraction is high (above 0.2-0.3),
219 organic O/C tends to increase with increasing ALW volume fraction; the increasing trend was most significant for spring and
220 autumn, while less significant for winter (Fig. 3a, c, d). The area between the two black lines in Fig. 3a, c, d is dominated by
221 the influence of ALW. Elevated ALW facilitates heterogeneous uptake or aqueous processes and promotes the formation of
222 more oxidized organics, such as dicarboxylic acids, thus increases O/C.

223
224 When ALW volume fraction is low (below 0.2-0.3), organic O/C decreases with lower NR-PM₁ mass concentration, indicated
225 by the size of the scattered points; this was observed in spring, autumn, and winter. One reason might be that at extremely low
226 aerosol mass concentrations, new particle formation events frequently occur and smaller particles dominate size distribution
227 (Cai et al., 2017; Guo et al., 2014). During formation and initial growth of new particles, extremely low volatile organic
228 compounds with the highest O/C ratio dominate; while subsequent growth involves organics with higher volatility and lower
229 O/C ratio (Donahue et al., 2013; Ehn et al., 2014). As a result, particle organic O/C decreases with growth of aerosol mass
230 concentration during new particle formation and growth events. Another possibility is that increased aerosol mass often
231 coincides with diminished solar radiation which suppresses photochemistry and may decrease organic O/C. In addition, a
232 fraction of the particles during clean periods are transported from less populated mountain areas. During such long-range
233 transport, atmospheric oxidation can increase O/C. Low ALW volume fraction correlates with low NR-PM₁ mass loadings,
234 which makes it look like organic O/C is decreasing with increasing ALW volume fraction. Overall, the apparent opposite trends
235 during high and low ALW volume fraction periods can actually be explained by a competition between the opposite impact of
236 ALW and NR-PM₁ mass loadings on organic evolution. However, summer was an exception, where no obvious dependence
237 of organic O/C on ALW volume fraction or NR-PM₁ mass concentration was observed.

238
239 The competing effects of ALW volume fractions and NR-PM₁ mass concentrations on organic O/C were further confirmed by
240 comparing organic evolution during the high and low-ALW haze episodes. Fig. 4 shows two typical haze episodes in Beijing,
241 with more chemical and meteorological information given in Fig. S5. During the high-ALW episode, where ALW contributes
242 0.2 - 0.75 to the total aerosol volume, organic O/C increases with haze accumulation. The increase of nighttime O/C is more
243 striking than that of daytime, likely due to the more abundant ALW at night (see Fig. S4). On the contrary, during the low-
244 ALW episode, where ALW volume fraction does not exceed 30%, daytime organic O/C decreases despite the increasing ALW

245 and T ; this indicates that the decrease in O/C introduced by reduced photo-oxidation process and gas-particle partitioning is
246 larger than the O/C increase from heterogeneous uptake or aqueous processes. Nighttime O/C remains relatively constant,
247 suggesting that the promoting effect of heterogeneous uptake or aqueous processes on O/C is comparable to the reducing
248 effects on O/C.

249 **3.3 The influence of RH and particle hygroscopicity on particle hygroscopic volume growth factor**

250 Particle volume growth factor increases rapidly with RH and particle hygroscopicity (Fig. 5). When RH is less than 80%,
251 particle VGF increases slowly from 1 to 2.5 with rising RH; when RH exceeds 80%, VGF increases rapidly to above 5. This
252 is generally consistent with previous studies (Bian et al., 2014). As shown in Fig. 5, significant variation of κ_{total} also plays an
253 important role on the change of water uptake. The dispersion of points in the vertical direction represents the influence of
254 particle chemical compositions to ALW. For instance, when RH is fixed at 60%, VGF increases from 1.2 to 1.9 when κ_{total}
255 increases from ~ 0.20 to ~ 0.45 .

256
257 The seasonal variations also reflect a combined promoting effect of RH and κ_{total} on VGF. The average VGFs for spring,
258 summer, autumn, and winter are 1.4, 1.6, 1.3, and 1.3, respectively. The highest VGF in summer is attributed to a combination
259 of the higher frequency for high RH (red step line, compared to green, orange, and blue step line in Fig. 5b) and the relatively
260 high particle hygroscopicity, κ_{total} (0.35, compared to 0.38, 0.30, and 0.33 for other seasons).

261
262 A consequence of the high RH and high ALW is the higher particle overall hygroscopicity, κ_{total} , as compared with that at the
263 low RH (Fig. 5). Aerosols are dominated by less hygroscopic particles ($\kappa_{total} < 0.3$) for RH below $\sim 40\%$ while aerosols are
264 dominated by more hygroscopic particles ($\kappa_{total} > 0.4$) for RH above $\sim 80\%$ (Fig. 5). This suggests positive feedback between
265 overall particle hygroscopicity and ALW. Higher κ_{total} leads to higher ALW in similar RH while higher ALW, or higher RH, in
266 turn corresponds to higher κ_{total} .

267 **3.4 Interactions between organic evolution and particle hygroscopicity during high and low-haze** 268 **episodes**

269 During high-ALW episodes, the organic volume fraction decreases and organic hygroscopicity increases substantially during
270 the accumulation of pollution. The average $frac_{org}$ is 0.51 and the daily increment of $frac_{org}$ is -11% (Fig. 6). The negative
271 $frac_{org}$ increment indicates decreasing $frac_{org}$ which reflects the larger increase of inorganic soluble compounds (sulfate, nitrate,
272 ammonium, and chloride) compared to that of organics during haze episodes. The average κ_{org} is 0.165 and the relative daily
273 increment of κ_{org} is 8%. The positive κ_{org} increment during high-ALW episodes reflects increasing κ_{org} due to the effect of

274 heterogeneous uptake or aqueous processes. To sum up, although the organic fraction decreases during the high-ALW haze
275 episodes, the organic hygroscopicity increases. As a result, the contribution of ALW_{org} to total ALW does not decrease as fast
276 as the decrease of organic fraction.

277
278 During low-ALW episodes, the decrease in organic volume fraction is slower than that during high-ALW episodes, and organic
279 hygroscopicity is relatively stable in the haze evolution process. The average $frac_{org}$ is 0.63 and the daily increment of $frac_{org}$
280 is -4% (Fig. 6), of which both are higher than those in high-ALW episodes. This suggests that organic is still the dominating
281 component as haze accumulated during low-ALW episodes. The average κ_{org} is 0.152 and the relative daily increment of κ_{org} is
282 -1%, both of which are lower than those in high-ALW episodes. The near zero increment of κ_{org} is a consequence of the
283 competition between heterogeneous uptake or aqueous processes and other processes. To sum up, the effects of ALW on
284 chemical compositions during low-ALW episodes are limited compared to high-ALW episodes.

285
286 As a consequence of the more significant changes in chemical composition during high-ALW episodes, the increase in particle
287 hygroscopicity is larger for high-ALW episodes than for low-ALW episodes. The relative daily increments of $frac_{org} \cdot \kappa_{org}$ during
288 high-ALW and low-ALW episodes are -4% and -3%, respectively (Fig. 6c). These negative increments indicate the negative
289 effect of the organic hygroscopic term on κ_{total} during haze episodes. For high-ALW episodes, this means that the increase in
290 organic hygroscopicity in high-ALW episodes does not compensate for the effect of decreasing organic fraction. However, the
291 average daily increments of κ_{total} during high-ALW and low-ALW haze episode are 8% and 2%, respectively (Fig. 6d). As κ_{inorg}
292 is fixed to 0.6 and the increment of $frac_{inorg}$ is opposite to that of $frac_{org}$, the positive κ_{total} increment is a result of the positive
293 increment of the term $frac_{inorg} \cdot \kappa_{inorg}$.

294
295 The rapid decrease in $frac_{org}$ and increase in κ_{org} during high-ALW episodes increase κ_{total} , which in turn promotes the ability
296 of particles to uptake water, forming positive feedbacks with ALW, as the conceptual diagram shows (Fig. 7). The decrease of
297 $frac_{org}$ or increase of $frac_{inorg}$ plays a dominating role while the increase in κ_{org} plays a minor but non-negligible role in
298 increasing κ_{total} . During low-ALW episodes, the positive feedbacks are weak or does not exist because both $frac_{org}$ and κ_{org} do
299 not change significantly.

300
301 There are other factors, not taken into consideration here, that might also affect ALW. These factors include the presence of
302 crustal material or trace metals, detailed particle size distributions, interactions between inorganic and organic compounds,
303 organic surfactants, and the particle phase state (Bian et al., 2014; Fountoukis and Nenes, 2007; Nakao, 2017; Ovadnevaite et
304 al., 2017). As a result, we suggest that long term measurements of ALW and κ_{org} should be performed to test the results shown
305 here and to establish a more reliable and accurate relationship between organic properties and ALW in the real atmosphere.

306 4 Conclusion

307 Our study emphasizes the need to include aerosol liquid water contributed by organics (ALW_{org}) in ALW modelling in Beijing,
308 instead of only using the inorganic contribution to total ALW. The reason is that ALW_{org} contributes an average of 18-32% to
309 the total ALW in Beijing, according to our modelling results with ISORROPIA-II, κ -Köhler theory, and the ZSR mixing rule.
310 It is also necessary to use a real-time κ_{org} to evaluate ALW_{org} . Since organic O/C, which has been shown in previous studies to
311 have a linear relationship with κ_{org} , varies from 0.2 to 1.3 in different seasons in Beijing. Using a fixed κ_{org} (0.08) for typical
312 urban areas underestimates ALW_{org} by a factor of ~ 2 in Beijing. When real-time κ_{org} is not available, a localized average κ_{org}
313 should be used. O/C, or κ_{org} , generally increases with rising temperature and rising ALW in spring, autumn, and winter in
314 Beijing.

315
316 Positive feedback loops were found between κ_{total} (which was determined by $frac_{org}$ and κ_{org} , as κ_{inorg} was assumed to be 0.6)
317 and ALW during high-ALW episodes. During high-ALW haze episodes, RH, NR- PM_{10} , and ALW increase rapidly. The strong
318 heterogeneous uptake and aqueous processes lead to a rapid decrease in $frac_{org}$ and an increase in κ_{org} . These variations increase
319 κ_{total} , thus further promote the uptake of water and form positive feedbacks. These positive feedbacks were much weaker in
320 low-ALW episodes. The positive feedback loop between chemical composition evolution (mainly indicated by $frac_{org}$ and κ_{org})
321 and ALW during high ALW-episodes is a driver for the severe haze episodes in Beijing.

322 Acknowledgments

323 Financial support from the National Key R&D Program of China (2016YFC0200102) and the National Science Foundation of
324 China (91643201) is acknowledged.

325 Reference

- 326 Andreae, M. O., and Rosenfeld, D.: Aerosol-cloud-precipitation interactions. Part 1. The nature and sources of cloud-active
327 aerosols, *Earth-Sci Rev*, 89, 13-41, 2008.
- 328 Asa-Awuku, A., Nenes, A., Gao, S., Flagan, R., and Seinfeld, J. H.: Water-soluble SOA from Alkene ozonolysis: composition
329 and droplet activation kinetics inferences from analysis of CCN activity, *Atmos Chem Phys*, 10, 1585-1597, 2010.
- 330 Bassett, M., and Seinfeld, J. H.: ATMOSPHERIC EQUILIBRIUM-MODEL OF SULFATE AND NITRATE AEROSOLS,
331 *Atmos Environ*, 17, 2237-2252, 10.1016/0004-6981(83)90221-4, 1983.
- 332 Bian, Y., Zhao, C., Ma, N., Chen, J., and Xu, W.: A study of aerosol liquid water content based on hygroscopicity measurements
333 at high relative humidity in the North China Plain, *Atmos Chem Phys*, 14, 6417-6426, 2014.
- 334 Cai, R., and Jiang, J.: A new balance formula to estimate new particle formation rate: reevaluating the effect of coagulation

335 scavenging, *Atmos Chem Phys*, 17, 12659-12675, 2017.

336 Cai, R., Yang, D., Fu, Y., Wang, X., Li, X., Ma, Y., Hao, J., Zheng, J., and Jiang, J.: Aerosol surface area concentration: a
337 governing factor in new particle formation in Beijing, *Atmos Chem Phys*, 17, 12327, 2017.

338 Canagaratna, M. R., Jimenez, J. L., Kroll, J. H., Chen, Q., Kessler, S. H., Massoli, P., Hildebrandt Ruiz, L., Fortner, E., Williams,
339 L. R., Wilson, K. R., Surratt, J. D., Donahue, N. M., Jayne, J. T., and Worsnop, D. R.: Elemental ratio measurements of organic
340 compounds using aerosol mass spectrometry: characterization, improved calibration, and implications, *Atmos Chem Phys*, 15,
341 253-272, 10.5194/acp-15-253-2015, 2015.

342 Cao, C., Jiang, W., Wang, B., Fang, J., Lang, J., Tian, G., Jiang, J., and Zhu, T. F.: Inhalable microorganisms in Beijing's PM_{2.5}
343 and PM₁₀ pollutants during a severe smog event, *Environ Sci Technol*, 48, 1499-1507, 2014.

344 Carlton, A., Wiedinmyer, C., and Kroll, J.: A review of Secondary Organic Aerosol (SOA) formation from isoprene, *Atmos*
345 *Chem Phys*, 9, 4987-5005, 2009.

346 Chang, R.-W., Slowik, J., Shantz, N., Vlasenko, A., Liggio, J., Sjostedt, S., Leaitch, W., and Abbatt, J.: The hygroscopicity
347 parameter (κ) of ambient organic aerosol at a field site subject to biogenic and anthropogenic influences: relationship to degree
348 of aerosol oxidation, *Atmos Chem Phys*, 10, 5047-5064, 2010.

349 Cheng, Y., Zheng, G., Wei, C., Mu, Q., Zheng, B., Wang, Z., Gao, M., Zhang, Q., He, K., Carmichael, G., Poschl, U., and Su,
350 H.: Reactive nitrogen chemistry in aerosol water as a source of sulfate during haze events in China, *Science Advances*, 2,
351 10.1126/sciadv.1601530, 2016.

352 Cheng, Y. F., Wiedensohler, A., Eichler, H., Heintzenberg, J., Tesche, M., Ansmann, A., Wendisch, M., Su, H., Althausen, D.,
353 Herrmann, H., Gnauk, T., Brüeggemann, E., Hu, M., and Zhang, Y. H.: Relative humidity dependence of aerosol optical
354 properties and direct radiative forcing in the surface boundary layer at Xinken in Pearl River Delta of China: An observation
355 based numerical study, *Atmos Environ*, 42, 6373-6397, 10.1016/j.atmosenv.2008.04.009, 2008.

356 Clegg, S. L., and Pitzer, K. S.: Thermodynamics of multicomponent, miscible, ionic solutions: generalized equations for
357 symmetrical electrolytes, *The Journal of Physical Chemistry*, 96, 3513-3520, 1992.

358 Clegg, S. L., Pitzer, K. S., and Brimblecombe, P.: Thermodynamics of multicomponent, miscible, ionic solutions. Mixtures
359 including unsymmetrical electrolytes, *The Journal of Physical Chemistry*, 96, 9470-9479, 1992.

360 Covert, D. S., Charlson, R. J., and Ahlquist, N. C.: A study of the relationship of chemical composition and humidity to light
361 scattering by aerosols, *Journal of Applied Meteorology*, 11, 968-976, 10.1175/1520-0450(1972)011<0968:asotro>2.0.co;2,
362 1972.

363 Crenn, V., Sciare, J., Croteau, P. L., Verlhac, S., Froehlich, R., Belis, C. A., Aas, W., Aijala, M., Alastuey, A., Artinano, B.,
364 Baisnee, D., Bonnaire, N., Bressi, M., Canagaratna, M., Canonaco, F., Carbone, C., Cavalli, F., Coz, E., Cubison, M. J., Esser-
365 Gietl, J. K., Green, D. C., Gros, V., Heikkinen, L., Herrmann, H., Lunder, C., Minguillon, M. C., Mocnik, G., O'Dowd, C. D.,
366 Ovadnevaite, J., Petit, J. E., Petralia, E., Poulain, L., Priestman, M., Riffault, V., Ripoll, A., Sarda-Estevé, R., Slowik, J. G.,
367 Setyan, A., Wiedensohler, A., Baltensperger, U., Prevot, A. S. H., Jayne, J. T., and Favez, O.: ACTRIS ACSM intercomparison
368 - Part 1: Reproducibility of concentration and fragment results from 13 individual Quadrupole Aerosol Chemical Speciation
369 Monitors (Q-ACSM) and consistency with co-located instruments, *Atmos Meas Tech*, 8, 5063-5087, 10.5194/amt-8-5063-
370 2015, 2015.

371 Dick, W. D., Saxena, P., and McMurry, P. H.: Estimation of water uptake by organic compounds in submicron aerosols
372 measured during the Southeastern Aerosol and Visibility Study, *Journal of Geophysical Research: Atmospheres*, 105, 1471-
373 1479, 2000.

374 Donahue, N. M., Ortega, I. K., Chuang, W., Riipinen, I., Riccobono, F., Schobesberger, S., Dommen, J., Baltensperger, U.,
375 Kulmala, M., Worsnop, D. R., and Vehkamäki, H.: How do organic vapors contribute to new-particle formation?, *Faraday*
376 *discussions*, 165, 91-104, 10.1039/c3fd00046j, 2013.

377 Duplissy, J., DeCarlo, P. F., Dommen, J., Alfarra, M. R., Metzger, A., Barmapadimos, I., Prevot, A. S. H., Weingartner, E.,
378 Tritscher, T., Gysel, M., Aiken, A. C., Jimenez, J. L., Canagaratna, M. R., Worsnop, D. R., Collins, D. R., Tomlinson, J., and
379 Baltensperger, U.: Relating hygroscopicity and composition of organic aerosol particulate matter, *Atmos Chem Phys*, 11, 1155-
380 1165, 10.5194/acp-11-1155-2011, 2011.

381 Dusek, U., Frank, G. P., Curtius, J., Drewnick, F., Schneider, J., Kuerten, A., Rose, D., Andreae, M. O., Borrmann, S., and

382 Poeschl, U.: Enhanced organic mass fraction and decreased hygroscopicity of cloud condensation nuclei (CCN) during new
383 particle formation events, *Geophys Res Lett*, 37, 10.1029/2009gl040930, 2010.

384 Ehn, M., Thornton, J. A., Kleist, E., Sipila, M., Junninen, H., Pullinen, I., Springer, M., Rubach, F., Tillmann, R., Lee, B.,
385 Lopez-Hilfiker, F., Andres, S., Acir, I.-H., Rissanen, M., Jokinen, T., Schobesberger, S., Kangasluoma, J., Kontkanen, J.,
386 Nieminen, T., Kurtén, T., Nielsen, L. B., Jorgensen, S., Kjaergaard, H. G., Canagaratna, M., Dal Maso, M., Berndt, T., Petaja,
387 T., Wahner, A., Kerminen, V.-M., Kulmala, M., Worsnop, D. R., Wildt, J., and Mentel, T. F.: A large source of low-volatility
388 secondary organic aerosol, *Nature*, 506, 476-+, 10.1038/nature13032, 2014.

389 Engelhart, G. J., Hildebrandt, L., Kostenidou, E., Mihalopoulos, N., Donahue, N. M., and Pandis, S. N.: Water content of aged
390 aerosol, *Atmos Chem Phys*, 11, 911-920, 10.5194/acp-11-911-2011, 2011.

391 Ervens, B., Sorooshian, A., Lim, Y. B., and Turpin, B. J.: Key parameters controlling OH-initiated formation of secondary
392 organic aerosol in the aqueous phase (aqSOA), *J Geophys Res-Atmos*, 119, 3997-4016, 10.1002/2013jd021021, 2014.

393 Fajardo, O. A., Jiang, J., and Hao, J.: Continuous Measurement of Ambient Aerosol Liquid Water Content in Beijing, *Aerosol*
394 *Air Qual Res*, 16, 1152-1164, 10.4209/aaqr.2015.10.0579, 2016.

395 Fountoukis, C., and Nenes, A.: ISORROPIA II: a computationally efficient thermodynamic equilibrium model for K^+ - Ca^{2+} -
396 Mg^{2+} - NH_4^+ - Na^+ - SO_4^{2-} - NO_3^- - Cl^- - H_2O aerosols, *Atmos Chem Phys*, 7, 4639-4659, 2007.

397 Fröhlich, R., Crenn, V., Setyan, A., Belis, C. A., Canonaco, F., Favez, O., Riffault, V., Slowik, J. G., Aas, W., and Aijälä, M.:
398 ACTRIS ACSM intercomparison-Part 2: Intercomparison of ME-2 organic source apportionment results from 15 individual,
399 co-located aerosol mass spectrometers, 2015.

400 Gunthe, S. S., King, S. M., Rose, D., Chen, Q., Roldin, P., Farmer, D. K., Jimenez, J. L., Artaxo, P., Andreae, M. O., Martin,
401 S. T., and Pöschl, U.: Cloud condensation nuclei in pristine tropical rainforest air of Amazonia: size-resolved measurements
402 and modeling of atmospheric aerosol composition and CCN activity, *Atmos Chem Phys*, 9, 7551-7575, 2009.

403 Gunthe, S. S., Rose, D., Su, H., Garland, R. M., Achtert, P., Nowak, A., Wiedensohler, A., Kuwata, M., Takegawa, N., Kondo,
404 Y., Hu, M., Shao, M., Zhu, T., Andreae, M. O., and Pöschl, U.: Cloud condensation nuclei (CCN) from fresh and aged air
405 pollution in the megacity region of Beijing, *Atmos Chem Phys*, 11, 11023-11039, 2011.

406 Guo, H., Xu, L., Bougiatioti, A., Cerully, K. M., Capps, S. L., Hite, J. R., Jr., Carlton, A. G., Lee, S. H., Bergin, M. H., Ng, N.
407 L., Nenes, A., and Weber, R. J.: Fine-particle water and pH in the southeastern United States, *Atmos Chem Phys*, 15, 5211-
408 5228, 10.5194/acp-15-5211-2015, 2015.

409 Guo, S., Hu, M., Zamora, M. L., Peng, J., Shang, D., Zheng, J., Du, Z., Wu, Z., Shao, M., and Zeng, L.: Elucidating severe
410 urban haze formation in China, *Proceedings of the National Academy of Sciences*, 111, 17373-17378, 2014.

411 He, K., Yang, F., Ma, Y., Zhang, Q., Yao, X., Chan, C. K., Cadle, S., Chan, T., and Mulawa, P.: The characteristics of PM_{2.5}
412 in Beijing, China, *Atmos Environ*, 35, 4959-4970, 2001.

413 Hennigan, C. J., Bergin, M. H., Dibb, J. E., and Weber, R. J.: Enhanced secondary organic aerosol formation due to water
414 uptake by fine particles, *Geophys Res Lett*, 35, 2008.

415 Hu, W., Hu, M., Hu, W., Jimenez, J. L., Yuan, B., Chen, W., Wang, M., Wu, Y., Chen, C., and Wang, Z.: Chemical composition,
416 sources, and aging process of submicron aerosols in Beijing: Contrast between summer and winter, *Journal of Geophysical*
417 *Research: Atmospheres*, 121, 1955-1977, 2016.

418 Huang, R.-J., Zhang, Y., Bozzetti, C., Ho, K.-F., Cao, J.-J., Han, Y., Daellenbach, K. R., Slowik, J. G., Platt, S. M., and
419 Canonaco, F.: High secondary aerosol contribution to particulate pollution during haze events in China, *Nature*, 514, 218-222,
420 2014.

421 Jia, Y., Rahn, K. A., He, K., Wen, T., and Wang, Y.: A novel technique for quantifying the regional component of urban aerosol
422 solely from its sawtooth cycles, *J Geophys Res-Atmos*, 113, 10.1029/2008jd010389, 2008.

423 Jimenez, J. L., Canagaratna, M. R., Donahue, N. M., Prevot, A. S. H., Zhang, Q., Kroll, J. H., DeCarlo, P. F., Allan, J. D., Coe,
424 H., Ng, N. L., Aiken, A. C., Docherty, K. S., Ulbrich, I. M., Grieshop, A. P., Robinson, A. L., Duplissy, J., Smith, J. D., Wilson,
425 K. R., Lanz, V. A., Hueglin, C., Sun, Y. L., Tian, J., Laaksonen, A., Raatikainen, T., Rautiainen, J., Vaattovaara, P., Ehn, M.,
426 Kulmala, M., Tomlinson, J. M., Collins, D. R., Cubison, M. J., Dunlea, E. J., Huffman, J. A., Onasch, T. B., Alfarra, M. R.,
427 Williams, P. I., Bower, K., Kondo, Y., Schneider, J., Drewnick, F., Borrmann, S., Weimer, S., Demerjian, K., Salcedo, D.,
428 Cottrell, L., Griffin, R., Takami, A., Miyoshi, T., Hatakeyama, S., Shimono, A., Sun, J. Y., Zhang, Y. M., Dzepina, K., Kimmel,

429 J. R., Sueper, D., Jayne, J. T., Herndon, S. C., Trimborn, A. M., Williams, L. R., Wood, E. C., Middlebrook, A. M., Kolb, C.
430 E., Baltensperger, U., and Worsnop, D. R.: Evolution of Organic Aerosols in the Atmosphere, *Science*, 326, 1525-1529,
431 10.1126/science.1180353, 2009.

432 Jing, B., Wang, Z., Tan, F., Guo, Y., Tong, S., Wang, W., Zhang, Y., and Ge, M.: Hygroscopic behavior of atmospheric aerosols
433 containing nitrate salts and water-soluble organic acids, *Atmos Chem Phys*, 18, 5115-5127, 10.5194/acp-18-5115-2018, 2018.

434 Kim, Y. P., Seinfeld, J. H., and Saxena, P.: Atmospheric gas-aerosol equilibrium I. Thermodynamic model, *Aerosol Sci Tech*,
435 19, 157-181, 1993a.

436 Kim, Y. P., Seinfeld, J. H., and Saxena, P.: Atmospheric gas-aerosol equilibrium II. Analysis of common approximations and
437 activity coefficient calculation methods, *Aerosol Sci Tech*, 19, 182-198, 1993b.

438 Lambe, A. T., Onasch, T. B., Massoli, P., Croasdale, D. R., Wright, J. P., Ahern, A. T., Williams, L. R., Worsnop, D. R., Brune,
439 W. H., and Davidovits, P.: Laboratory studies of the chemical composition and cloud condensation nuclei (CCN) activity of
440 secondary organic aerosol (SOA) and oxidized primary organic aerosol (OPOA), *Atmos Chem Phys*, 11, 8913-8928,
441 10.5194/acp-11-8913-2011, 2011.

442 Liu, H. J., Zhao, C. S., Nekat, B., Ma, N., Wiedensohler, A., van Pinxteren, D., Spindler, G., Mueller, K., and Herrmann, H.:
443 Aerosol hygroscopicity derived from size-segregated chemical composition and its parameterization in the North China Plain,
444 *Atmos Chem Phys*, 14, 2525-2539, 10.5194/acp-14-2525-2014, 2014.

445 Liu, X. G., Sun, K., Qu, Y., Hu, M., Sun, Y. L., Zhang, F., and Zhang, Y. H.: Secondary Formation of Sulfate and Nitrate during
446 a Haze Episode in Megacity Beijing, China, *Aerosol Air Qual Res*, 15, 2246-2257, 10.4209/aaqr.2014.12.0321, 2015.

447 Liu, Y., Wu, Z., Wang, Y., Xiao, Y., Gu, F., Zheng, J., Tan, T., Shang, D., Wu, Y., Zeng, L., Hu, M., Bateman, A. P., and Martin,
448 S. T.: Submicrometer Particles Are in the Liquid State during Heavy Haze Episodes in the Urban Atmosphere of Beijing, China,
449 *Environ Sci Tech Lett*, 4, 427-432, 10.1021/acs.estlett.7b00352, 2017.

450 Löndahl, J., Pagels, J., Boman, C., Swietlicki, E., Massling, A., Rissler, J., Blomberg, A., Bohgard, M., and Sandström, T.:
451 Deposition of biomass combustion aerosol particles in the human respiratory tract, *Inhalation toxicology*, 20, 923-933, 2008.

452 Martin, S. T., Rosenoern, T., Chen, Q., and Collins, D. R.: Phase changes of ambient particles in the Southern Great Plains of
453 Oklahoma, *Geophys Res Lett*, 35, 2008.

454 Massoli, P., Lambe, A., Ahern, A., Williams, L., Ehn, M., Mikkilä, J., Canagaratna, M., Brune, W., Onasch, T., and Jayne, J.:
455 Relationship between aerosol oxidation level and hygroscopic properties of laboratory generated secondary organic aerosol
456 (SOA) particles, *Geophys Res Lett*, 37, 2010.

457 Nakao, S.: Why would apparent κ linearly change with O/C? Assessing the Role of Volatility, Solubility, and Surface Activity
458 of Organic Aerosols, *Aerosol Sci Tech*, 1-12, 2017.

459 Nenes, A., Pandis, S. N., and Pilinis, C.: ISORROPIA: A new thermodynamic equilibrium model for multiphase
460 multicomponent inorganic aerosols, *Aquatic geochemistry*, 4, 123-152, 1998.

461 Nenes, A., Pandis, S. N., and Pilinis, C.: Continued development and testing of a new thermodynamic aerosol module for
462 urban and regional air quality models, *Atmos Environ*, 33, 1553-1560, 1999.

463 Ng, N. L., Canagaratna, M. R., Zhang, Q., Jimenez, J. L., Tian, J., Ulbrich, I. M., Kroll, J. H., Docherty, K. S., Chhabra, P. S.,
464 Bahreini, R., Murphy, S. M., Seinfeld, J. H., Hildebrandt, L., Donahue, N. M., DeCarlo, P. F., Lanz, V. A., Prevot, A. S. H.,
465 Dinar, E., Rudich, Y., and Worsnop, D. R.: Organic aerosol components observed in Northern Hemispheric datasets from
466 Aerosol Mass Spectrometry, *Atmos Chem Phys*, 10, 4625-4641, 10.5194/acp-10-4625-2010, 2010.

467 Ng, N. L., Herndon, S. C., Trimborn, A., Canagaratna, M. R., Croteau, P. L., Onasch, T. B., Sueper, D., Worsnop, D. R., Zhang,
468 Q., Sun, Y. L., and Jayne, J. T.: An Aerosol Chemical Speciation Monitor (ACSM) for Routine Monitoring of the Composition
469 and Mass Concentrations of Ambient Aerosol, *Aerosol Sci Tech*, 45, 780-794, 2011.

470 Nguyen, T. K. V., Zhang, Q., Jimenez, J. L., Pike, M., and Carlton, A. G.: Liquid Water: Ubiquitous Contributor to Aerosol
471 Mass, *Environ Sci Tech Lett*, 3, 257-263, 10.1021/acs.estlett.6b00167, 2016.

472 Ovadnevaite, J., Zuend, A., Laaksonen, A., Sanchez, K. J., Roberts, G., Ceburnis, D., Decesari, S., Rinaldi, M., Hodas, N., and
473 Facchini, M. C.: Surface tension prevails over solute effect in organic-influenced cloud droplet activation, *Nature*, 546, 637,
474 2017.

475 Parikh, H. M., Carlton, A. G., Vizuete, W., and Kamens, R. M.: Modeling secondary organic aerosol using a dynamic

476 partitioning approach incorporating particle aqueous-phase chemistry, *Atmos Environ*, 45, 1126-1137, 2011.

477 Peter, T., Marcolli, C., Spichtinger, P., Corti, T., Baker, M. B., and Koop, T.: When dry air is too humid, *Science*, 314, 1399-

478 1402, 2006.

479 Petters, M., Wex, H., Carrico, C., Hallbauer, E., Massling, A., McMeeking, G., Poulain, L., Wu, Z., Kreidenweis, S., and

480 Stratmann, F.: Towards closing the gap between hygroscopic growth and activation for secondary organic aerosol—Part 2:

481 Theoretical approaches, *Atmos Chem Phys*, 9, 3999-4009, 2009.

482 Petters, M. D., and Kreidenweis, S. M.: A single parameter representation of hygroscopic growth and cloud condensation

483 nucleus activity, *Atmos Chem Phys*, 7, 1961-1971, 2007.

484 Pilinis, C., Seinfeld, J. H., and Grosjean, D.: WATER-CONTENT OF ATMOSPHERIC AEROSOLS, *Atmos Environ*, 23,

485 1601-1606, 10.1016/0004-6981(89)90419-8, 1989.

486 Quan, J., Liu, Q., Li, X., Gao, Y., Jia, X., Sheng, J., and Liu, Y.: Effect of heterogeneous aqueous reactions on the secondary

487 formation of inorganic aerosols during haze events, *Atmos Environ*, 122, 306-312, 10.1016/j.atmosenv.2015.09.068, 2015.

488 Raatikainen, T., Vaattovaara, P., Tiitta, P., Miettinen, P., Rautiainen, J., Ehn, M., Kulmala, M., Laaksonen, A., and Worsnop, D.

489 R.: Physicochemical properties and origin of organic groups detected in boreal forest using an aerosol mass spectrometer,

490 *Atmos Chem Phys*, 10, 2063-2077, 10.5194/acp-10-2063-2010, 2010.

491 Rader, D., and McMurry, P.: Application of the tandem differential mobility analyzer to studies of droplet growth or evaporation,

492 *J Aerosol Sci*, 17, 771-787, 1986.

493 Rood, M., Shaw, M., Larson, T., and Covert, D.: Ubiquitous nature of ambient metastable aerosol, *Nature*, 337, 537-539, 1989.

494 Rose, D., Gunthe, S. S., Su, H., Garland, R. M., Yang, H., Berghof, M., Cheng, Y. F., Wehner, B., Achtert, P., Nowak, A.,

495 Wiedensohler, A., Takegawa, N., Kondo, Y., Hu, M., Zhang, Y., Andreae, M. O., and Poeschl, U.: Cloud condensation nuclei

496 in polluted air and biomass burning smoke near the mega-city Guangzhou, China -Part 2: Size-resolved aerosol chemical

497 composition, diurnal cycles, and externally mixed weakly CCN-active soot particles, *Atmos Chem Phys*, 11, 2817-2836,

498 10.5194/acp-11-2817-2011, 2011.

499 Salcedo, D., Onasch, T. B., Dzepina, K., Canagaratna, M. R., Zhang, Q., Huffman, J. A., DeCarlo, P. F., Jayne, J. T., Mortimer,

500 P., Worsnop, D. R., Kolb, C. E., Johnson, K. S., Zuberi, B., Marr, L. C., Volkamer, R., Molina, L. T., Molina, M. J., Cardenas,

501 B., Bernabe, R. M., Marquez, C., Gaffney, J. S., Marley, N. A., Laskin, A., Shutthanandan, V., Xie, Y., Brune, W., Leshner, R.,

502 Shirley, T., and Jimenez, J. L.: Characterization of ambient aerosols in Mexico City during the MCMA-2003 campaign with

503 Aerosol Mass Spectrometry: results from the CENICA Supersite, *Atmos Chem Phys*, 6, 925-946, 2006.

504 Sievering, H., Boatman, J., Galloway, J., Keene, W., Kim, Y., Luria, M., and Ray, J.: Heterogeneous sulfur conversion in sea-

505 salt aerosol particles: the role of aerosol water content and size distribution, *Atmospheric Environment. Part A. General Topics*,

506 25, 1479-1487, 1991.

507 Song, S., Gao, M., Xu, W., Shao, J., Shi, G., Wang, S., Wang, Y., Sun, Y., and McElroy, M. B.: Fine-particle pH for Beijing

508 winter haze as inferred from different thermodynamic equilibrium models, *Atmos Chem Phys*, 18, 7423-7438, 10.5194/acp-

509 18-7423-2018, 2018.

510 Song, S., Gao, M., Xu, W., Sun, Y., Worsnop, D. R., Jayne, J. T., Zhang, Y., Zhu, L., Li, M., Zhou, Z., Cheng, C., Lv, Y., Wang,

511 Y., Peng, W., Xu, X., Lin, N., Wang, Y., Wang, S., Munger, J. W., Jacob, D. J., and McElroy, M. B.: Possible heterogeneous

512 chemistry of hydroxymethanesulfonate (HMS) in northern China winter haze, *Atmos Chem Phys*, 19, 1357-1371, 10.5194/acp-

513 19-1357-2019, 2019.

514 Stanier, C. O., Khlystov, A. Y., Chan, W. R., Mandiro, M., and Pandis, S. N.: A Method for the In Situ Measurement of Fine

515 Aerosol Water Content of Ambient Aerosols: The Dry-Ambient Aerosol Size Spectrometer (DAASS) Special Issue of *Aerosol*

516 *Science and Technology on Findings from the Fine Particulate Matter Supersites Program*, *Aerosol Sci Tech*, 38, 215-228,

517 2004.

518 Su, H., Rose, D., Cheng, Y. F., Gunthe, S. S., Massling, A., Stock, M., Wiedensohler, A., Andreae, M. O., and Poeschl, U.:

519 Hygroscopicity distribution concept for measurement data analysis and modeling of aerosol particle mixing state with regard

520 to hygroscopic growth and CCN activation, *Atmos Chem Phys*, 10, 7489-7503, 10.5194/acp-10-7489-2010, 2010.

521 Sun, Y., Du, W., Fu, P., Wang, Q., Li, J., Ge, X., Zhang, Q., Zhu, C., Ren, L., Xu, W., Zhao, J., Han, T., Worsnop, D. R., and

522 Wang, Z.: Primary and secondary aerosols in Beijing in winter: sources, variations and processes, *Atmos. Chem. Phys.*, 16,

8309-8329, 10.5194/acp-16-8309-2016, 2016.

Sun, Y. L., Wang, Z. F., Fu, P. Q., Jiang, Q., Yang, T., Li, J., and Ge, X. L.: The impact of relative humidity on aerosol composition and evolution processes during wintertime in Beijing, China, *Atmos Environ*, 77, 927-934, 10.1016/j.atmosenv.2013.06.019, 2013.

Topping, D., McFiggans, G., and Coe, H.: A curved multi-component aerosol hygroscopicity model framework: Part 2—Including organic compounds, *Atmos Chem Phys*, 5, 1223-1242, 2005a.

Topping, D., McFiggans, G., and Coe, H.: A curved multi-component aerosol hygroscopicity model framework: Part 1—Inorganic compounds, *Atmos Chem Phys*, 5, 1205-1222, 2005b.

Wang, G., Zhang, R., Gomez, M. E., Yang, L., Zamora, M. L., Hu, M., Lin, Y., Peng, J., Guo, S., and Meng, J.: Persistent sulfate formation from London Fog to Chinese haze, *Proceedings of the National Academy of Sciences*, 113, 13630-13635, 2016.

Wang, J., Shilling, J. E., Liu, J., Zelenyuk, A., Bell, D. M., Petters, M. D., Thalman, R., Mei, F., Zaveri, R. A., and Zheng, G.: Cloud droplet activation of secondary organic aerosol is mainly controlled by molecular weight, not water solubility, *Atmos. Chem. Phys.*, 19, 941-954, 10.5194/acp-19-941-2019, 2019.

Wu, Z., Wang, Y., Tan, T., Zhu, Y., Li, M., Shang, D., Wang, H., Lu, K., Guo, S., and Zeng, L.: Aerosol Liquid Water Driven by Anthropogenic Inorganic Salts: Implying Its Key Role in Haze Formation over the North China Plain, *Environ Sci Tech Lett*, 5, 160-166, 2018.

Xu, W., Han, T., Du, W., Wang, Q., Chen, C., Zhao, J., Zhang, Y., Li, J., Fu, P., and Wang, Z.: Effects of Aqueous-Phase and Photochemical Processing on Secondary Organic Aerosol Formation and Evolution in Beijing, China, *Environ Sci Technol*, 51, 762-770, 2017.

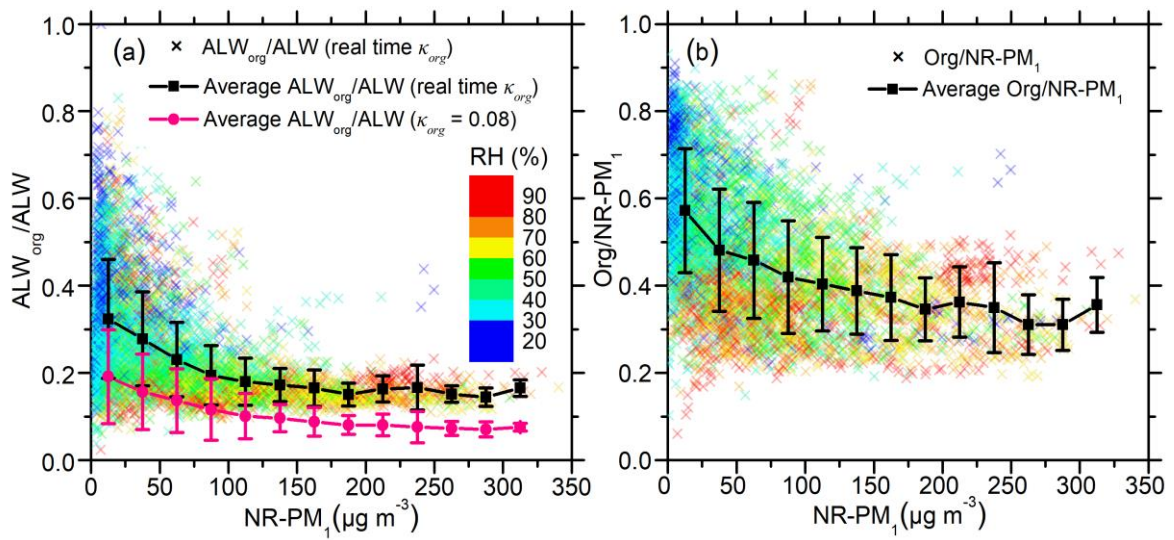
Zhang, Q., Jimenez, J. L., Canagaratna, M. R., Allan, J. D., Coe, H., Ulbrich, I., Alfarra, M. R., Takami, A., Middlebrook, A. M., Sun, Y. L., Dzepina, K., Dunlea, E., Docherty, K., DeCarlo, P. F., Salcedo, D., Onasch, T., Jayne, J. T., Miyoshi, T., Shimojo, A., Hatakeyama, S., Takegawa, N., Kondo, Y., Schneider, J., Drewnick, F., Borrmann, S., Weimer, S., Demerjian, K., Williams, P., Bower, K., Bahreini, R., Cottrell, L., Griffin, R. J., Rautiainen, J., Sun, J. Y., Zhang, Y. M., and Worsnop, D. R.: Ubiquity and dominance of oxygenated species in organic aerosols in anthropogenically-influenced Northern Hemisphere midlatitudes, *Geophys Res Lett*, 34, 2007.

Zheng, G., Duan, F., Ma, Y., Zhang, Q., Huang, T., Kimoto, T., Cheng, Y., Su, H., and He, K.: Episode-Based Evolution Pattern Analysis of Haze Pollution: Method Development and Results from Beijing, China, *Environ Sci Technol*, 50, 4632-4641, 10.1021/acs.est.5b05593, 2016.

Zheng, G. J., Duan, F. K., Su, H., Ma, Y. L., Cheng, Y., Zheng, B., Zhang, Q., Huang, T., Kimoto, T., Chang, D., Poeschl, U., Cheng, Y. F., and He, K. B.: Exploring the severe winter haze in Beijing: the impact of synoptic weather, regional transport and heterogeneous reactions, *Atmos Chem Phys*, 15, 2969-2983, 10.5194/acp-15-2969-2015, 2015.

555

556



557

558

559

560

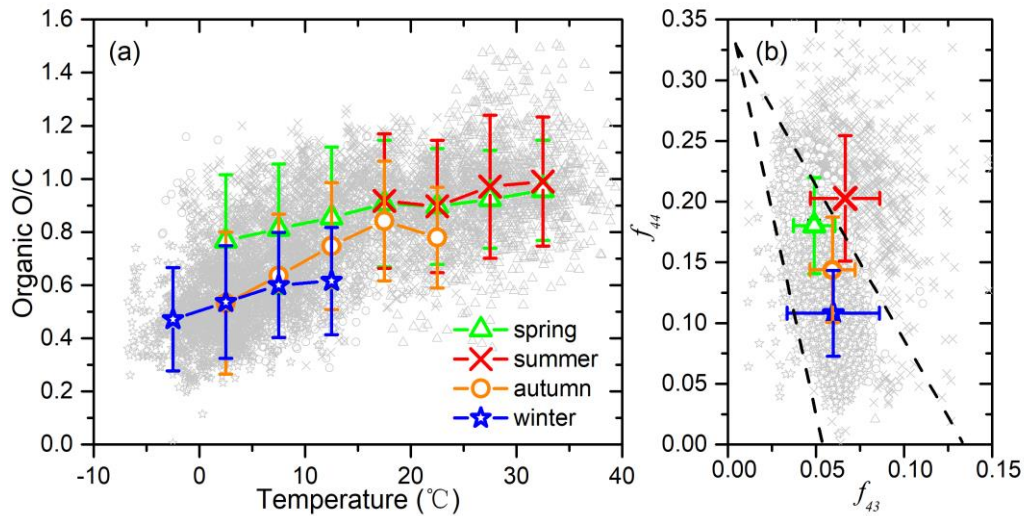
561

562

563

564

Figure 1. (a) The colored scatter points represent the fraction of aerosol liquid water contributed by organics (ALW_{org}/ALW), which was calculated using real-time κ_{org} . The black line shows the average of the colored points in each $NR-PM_1$ mass concentration bin. The pink line is the average ALW_{org}/ALW calculated using a fixed κ_{org} (0.08) in each $NR-PM_1$ mass concentration bin. (b) The colored scatter points represent the organic mass fraction in non-refractory submicron aerosol ($NR-PM_1$). The black line is the average of the colored points in each $NR-PM_1$ mass concentration bin. All the scattered points in both figures are colored with relative humidity (RH).



565

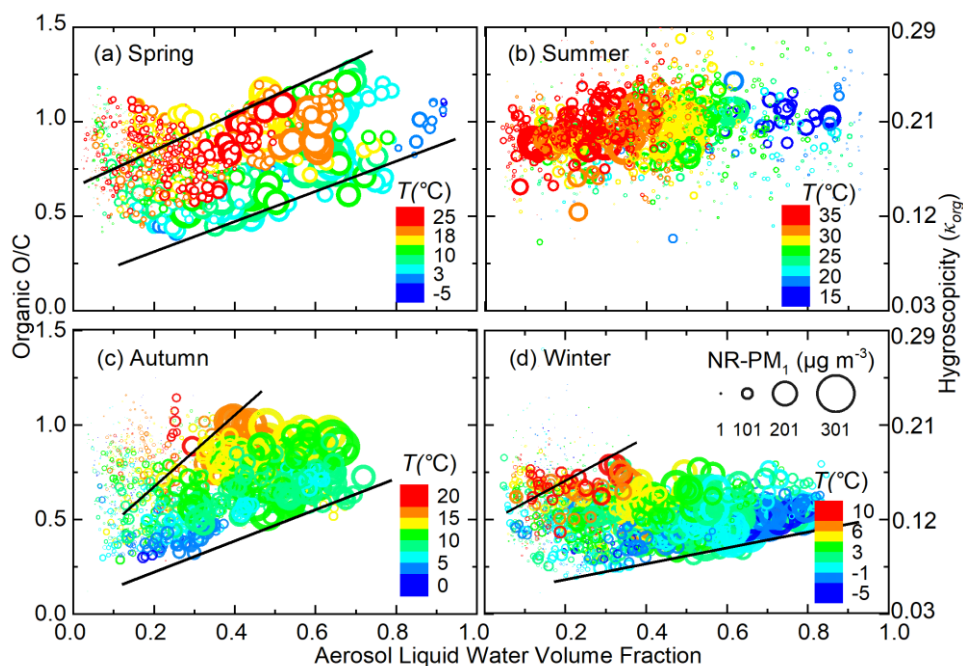
566

567

568

569

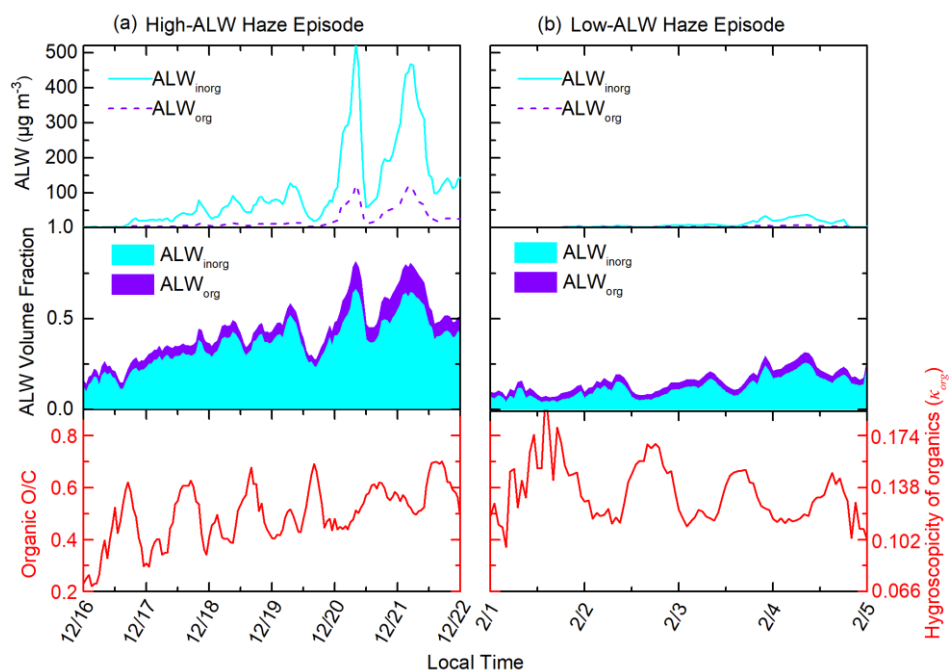
Figure 2. (a) O/C ratio as a function of temperature in different seasons of Beijing; (b) triangle plot (f_{44} vs f_{43}) measured by the Q-ACSM in different seasons of Beijing



570

571 **Figure 3. Variation of organic O/C ratio (calculated from Q-ACSM measured f_{44}) as a function of aerosol liquid water (ALW) volume**
 572 **fraction in different seasons of Beijing. The size and color of the points represent the corresponding NR-PM₁ mass concentration**
 573 **and ambient temperature, respectively. For spring, autumn, and winter, the areas between the two black lines represent the points**
 574 **less affected by the gas-particle partitioning under low aerosol mass loadings.**

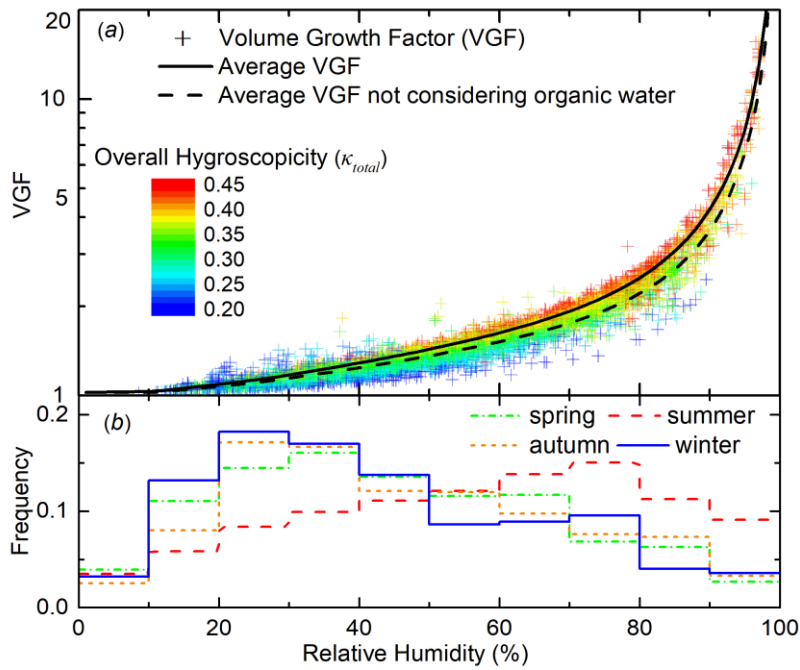
575



576

577 **Figure 4. Variations of aerosol liquid water contributed by organics (ALW_{org}), aerosol liquid water contributed by inorganics**
 578 **(ALW_{inorg}), the volume fraction of total wet particle compositions, organic O/C during (a) a typical high-ALW episode and (b) a**
 579 **typical low-ALW episode.**

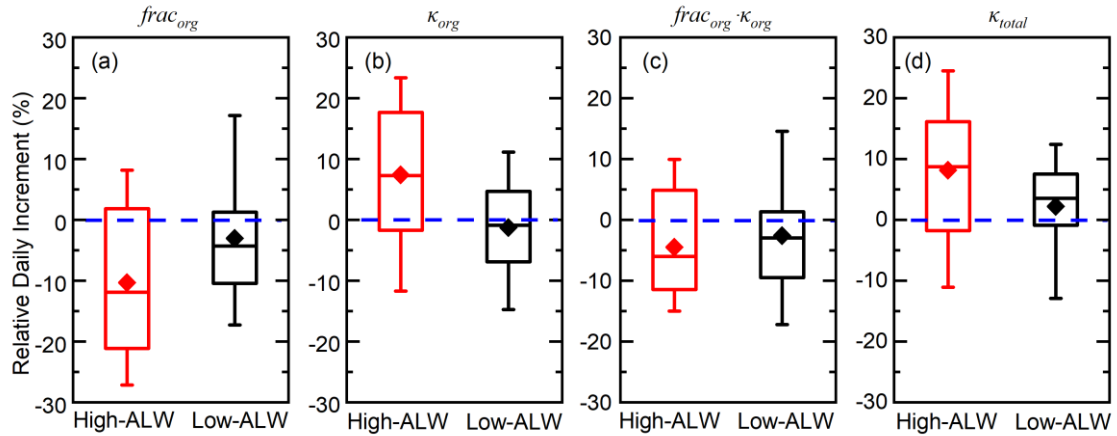
580



581

582 **Figure 5. (a) Volume growth factor (VGF, scattered points, calculated by Eq. 3) from the four seasons as a function of relative**
 583 **humidity (RH). The points are colored by overall particle hygroscopicity (κ_{total}) calculated from aerosol bulk composition (Eq. 4).**
 584 **The black line is the averaged VGF in different RH. Black dashed line is the average VGF without considering organic water. (b)**
 585 **RH frequency during four seasons is expressed in step line.**

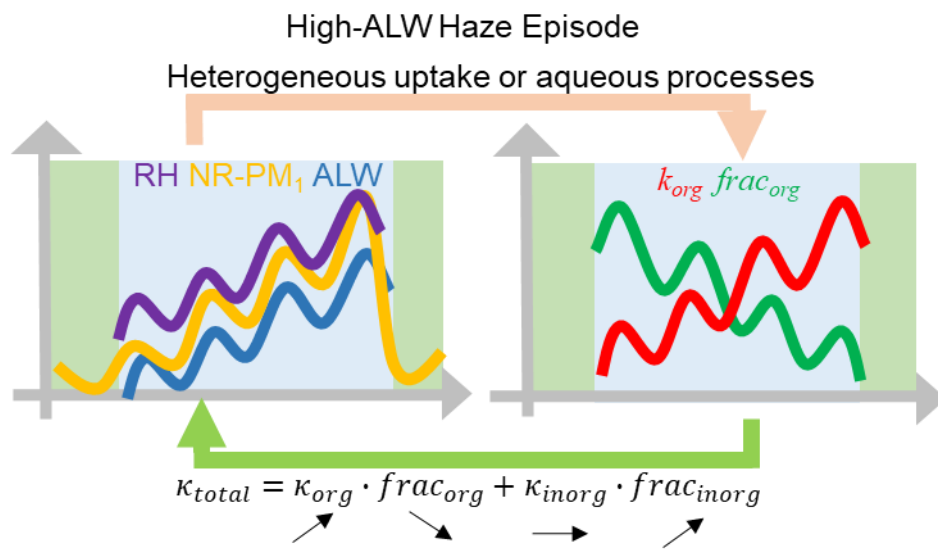
586



587

588 **Figure 6. Episode-based relative day increment of organic hygroscopicity (κ_{org}), organic volume fraction ($frac_{org}$), the hygroscopicity**
 589 **term contributed by organics ($\kappa_{org} \cdot frac_{org}$), and overall particle hygroscopicity (κ_{total}) during high-ALW haze episodes and low-ALW**
 590 **haze episodes. The box plots represent the 10th, 25th, 50th, 75th, and 90th percentiles of the corresponding data. The rhombus**
 591 **represents the mean value of the corresponding data.**

592



593

594

Figure 7. The positive feedback loops between aerosol liquid water and organic evolution during high-ALW haze episodes in Beijing.

595